arXiv:1910.00427v1 [gr-qc] 30 Sep 2019

Relativistic strange stars in Tolman-Kuchowicz spacetime

Suparna Biswas[a], Dibyendu Shee[b], Saibal Ray[b,c1], F. Rahaman[d], B.K. Guha[a]

[a] *Department of Physics, Indian Institute of Engineering Science and Technology, Shibpur, Howrah 711103, India*
[b] *Department of Physics, Government College of Engineering and Ceramic Technology, Kolkata 700010, West Bengal, India*
[c] *Department of Natural Sciences, Maulana Abul Kalam Azad University of Technology, Haringhata 741249, West Bengal, India*
[d] *Department of Mathematics, Jadavpur University, Kolkata 700032, West Bengal, India*

1. Introduction

Einstein's theory of General Relativity (GR) [3] is undoubtedly and undebatedly the most promising theory of the last century. Though the spark of Albert Einstein was proved by his theory of Special Relativity (SR) [4] in front of the entire world, whose generalisation leads us the former one. Einstein revealed the mysteries of the universe through complex calculation of Tensor Analysis and explained the beautiful philosophical concept that matter creates curvature in the spacetime [5]. Though, before Einstein's revolutionary discovery, tensor analysis was considered just as a mathematical tool, not so useful in physics. Even the concept of gravitational waves was also given by this theoretical physicist with his mastermind thinking, at that time of minimum technology. Einstein's field equations (EFE) for the spacetime is very essential to interpret various astrophysical phenomena like black holes, compact objects, supernovae and the formation of structure of the universe. After 100 years of GR, we are now able to detect gravitational

[1]*Corresponding author.
E-mail addresses: sb.rs2016@physics.iiests.ac.in (SB), dibyendu_shee@yahoo.com (DS), saibal@associates.iucaa.in (SR), rahaman@associates.iucaa.in (FR), dean.fa@iiests.ac.in (BKG).

waves by promising astronomical instruments like LIGO, LISA, Virgo etc. In a short, his creation made a new island of perambulation for the researchers in the field of astrophysics and cosmology.

After all the thermonuclear fuels burnt out, type II supernovae explosion occurs and the gravitational collapse of massive stars ($M > 8M_{\odot}$) gives the birth of neutron stars [6]. The concept of neutron stars got concrete support with the discovery of neutron particle in 1932 by Chadwick. Later, observationally detection of pulsars [7] strongly re-establish this concept. Being mostly dominated by neutron particle, neutron stars are extensively dense and even can distort the geometry of the spacetime. Their expanse is not very big, radius lies between $(11 - 15)$ km with mass $(1.4 - 2)$ $M_{\odot}$ [8]. Duncan and Thompson [9] suggest that strong magnetic field is a characteristic of such highly compact stars. An immense magnetic field of the order of 10^{14}-10^{15} Gauss can exist near the surface of the magnetars, strongly magnetized neutron stars [10, 11]. Later, Chakraborty et al. [12] suggest that, in the core of the neutron star even stronger magnetic field upto 10^{19}-10^{20} Gauss can potentially occur. Obviously the reason behind this strong magnetic field is still under discussion. Though spontaneous ordering of nucleon [13, 14] or quark spins [15] in the dense interior of a neutron star can be taken as a cause behind this debating issue.

The extreme high density and tremendous pressure at the core of the neutron star make it an object of various physical speculation among the astrophysicists. Due to this high density and pressure, there is a strong probability of phase transition of neutrons inside the neutron star to boson, hyperon and strange quark matter. The prediction of Cameron [16] tells us that hyperon must be produced inside the neutron star. Due to extreme high density and weak interaction, some of the nucleon may be converted into hyperon since this is energetically more favourable. Though interior of the neutron star may also contain quark matter. The quarks become free of interaction due to high density and extreme asymptotic momentum transfer at the core of the neutron star.

An individual nucleon contains quarks to form a colourless matter known as quark matter. The energy level of the hyperon at the Fermi-surface becomes higher than its rest mass, due to the tremendous density, as a result these particles could deconfine into strange quarks. The strange quarks are the most stable quarks. Though the quark stars consists of up (u), down (d) and strange (s) quarks but mostly it contain strange (s) quarks. Theoretically under certain conditions some of the u and d quarks transformed

into s quarks. As we know cold strange matter is the true ground state of nuclear matter [17, 18, 19, 20, 21], the up (u) and down (d) quarks once converted into strange matter, the entire quark matter get converted into strange matter. As a result the neutron star totally converted into strange quark star [22]. Some recent simulations [23, 24] pointed out the merger process of two strange stars. So their gravitational wave signal detection may enhance the probability of SQM hypothesis.

Since the quarks are not seen as free particles, the quark confinement mechanism have been dealt in Quantum Chromodynamics (QCD). A strongly interacting particle can be defined as a finite region of space, confined with fields [25]. Chodos et al. [25] described the Bag constant (B_g) as a finite region with constant energy density. So, the energy momentum tensor of the star must be effected by this constant, and thus the geometry of the spacetime also be influenced by the Bag constant. The MIT bag model states that the reason of quark confinement is due to the universal pressure B_g, known as the MIT bag constant, which is actually the difference between energy densities of the perturbative and nonperturbative quantum chromodynamical vacuum. For a stable strange quark matter, the proposed value of the Bag constant should be within the following range $(55 - 75)$ MeV/fm^3 [26, 21]. However, wide range of the Bag constant are permissible according to CERN-SPS and RHIC [27]. In a recent work Aziz et al. [28] have shown the possibility of wide range $(41.58 - 319.31)$ MeV/fm^3 for B_g which they have recovered from different observational data for several compact stars. The probable compact strange star candidates are $X-ray$ pulsars, viz. $Her\ X1$, millisecond pulsar $SAX\ J\ 1808.43658$, X ray sources, $4U\ 1820-30$ and $4U\ 1728-34$ etc.

Lugones and Abra$\tilde{n}$il [29] studied the structure of strange stars in Randall-Sundrum type II braneworld model and investigated the properties of hadronic and strange quark stars with the help of two typical EOSs, a nonlinear relativistic mean field model for hadronic matter and the MIT bag model for quark matter. Abra$\tilde{n}$il and Malheiro [30] studied radial stability of anisotropic strange quark stars, followed the MIT bag EOS, considering vanishing and nonvanishing effect of anisotropic factor at the surface of a strange star. Abbas et al. [31] studied the existence of strange stars in $f(T)$ modified gravity with the help of diagonal tetrad field of static spacetime with charged anisotropic fluid and MIT bag model. Isayev [32] studied the stability of magnetized strange quark matter (MSQM) using the MIT bag model with density dependent bag pressure. Paulucci and Horvath [33] presented an analysis of the fragmentation of SQM into strangelets (small lumps of

strange quark matter in which finite effects become important) [34, 35] in high temperature astrophysical events, considering quark matter within the MIT bag model framework in color-flavor-locked (CFL) state [36, 37, 38]. Deb et al. [39] studied ultra dense strange (quark) stars employing MIT bag model, assuming density profile as provided by Mak and Harko [40]. They featured an interesting result that anisotropy of highly compact strange stars increases with radial coordinate and attains its maximum value at the surface. This result seems to be an inherent property of the singularity free anisotropic strange stars. Rahaman et al. [41] studied anisotropic charged strange star in GR using MIT bag EOS, where B_g value becomes relatively higher probably to balance the excess repulsion, caused by electric field.

Recently, anisotropic strange star in modified $f(R,T)$ gravity has been investigated by Deb et al. [42] when the matter geometry coupling is simplest and minimum. They also studied isotropic case [43] in $f(R,T)$ gravity where they provided a stable stellar model to study strange stars. In our previous work [44], we have introduced a new model for highly compact anisotropic strange star using the metric potentials, given by Krori-Barua [45] under $f(R,T)$ gravity. We have calculated and explained an interesting result that value of the bag constant B_g reduces in $f(R,T)$ gravity due to the coupling effect between matter and geometry. Besides, there are so many more literatures [46, 47, 48, 49] available on strange stars based on MIT bag model EOS.

Depending on the inhomogeneity of matter distribution and its evolution, which also results anisotropic features, the fabric of spacetime of compact object changes. During the investigation of stellar properties we must have to keep in our mind that, for smaller radial size with higher density, anisotropic pressure plays an important role. The term anisotropic pressure signifies that the radial component of pressure (p_r) differ from that of tangential component of pressure (p_t). Actually Ruderman [50] has investigated the stellar models and argued that the nuclear matter may have anisotropic features at very high density ($> 10^{15}$ gm/cc), where the nuclear interaction must be treated relativistically. After this remarkable concept Bower and Liang [51], Bayin [52], Maharaj and Maartens [53] emphasised on the importance of locally anisotropic EOS for relativistic fluid spheres. Actually anisotropy affects the physical properties of a stellar object such as the radial pressure, total radius, total mass, energy density, surface redshift and the frequency of oscillation of the fundamental mode.

According to Kippenhahn and Weigert [54], the anisotropy may arises

due to presence of a type $3A$ superfluid or existence of solid stellar core. Sawyer [55] suggested that anisotropy in pressure may generate due to pion condensation. Another reason for anisotropy may be taken as different kind of phase transitions, according to Sokolov [56]. According to Weber [57] the immense magnetic field of neutron star may also produce anisotropy in pressure inside a strange star. Also the strong electric field produces the effect of anisotropy, as suggested by Usov [58]. The interior gravitational fields of anisotropic fluid spheres can be described properly by exact solutions of the EFE as shown in following references [59, 60, 61, 62, 63, 64, 65, 66, 67, 68, 69, 70, 71, 72, 73, 74].

To study the anisotropic strange star, we employ the TK metric potentials which provide a class of singularity free solution. Tolman in 1939 [1] independently gave analytical solutions of EFE by choosing eight different types of metric potentials. Also Kuchowicz in 1968 [2] independently gave this singularity-free metric potential to describe the stellar configuration.

Recently, Jasim et al. [75] presented a study on anisotropic strange star under the framework of Einstein's General Relativity by using the TK metric potentials. It is worthy to mention that their result provides theoretical support for massive strange stars for specific values of the model parameters. However, though flavour of MIT bag EOS is hidden in the value of B_g, the authors have considered the value for it arbitrarily. In connection to this aspect one may finds in literature [26, 21] that for stable SQM with the proposed range is $(55 - 75)$ MeV/fm^3.

Being motivated by the above background, especially from the work of Jasim et al. [75], here we have tried to introduce TK type metric potentials which provide us a singularity-free stellar model for a wide range of MIT bag values instead of a specific one. The scheme of the study is as follows: In Section 2 we have provided basic mathematical formulation of Einstein's spacetime. Section 3 contains solutions to the field equations. To represent the model properly we have found the numerical values of different model parameters, which are provided in Section 4. The physical features of our model are represented in Section 5 through various subsections, namely, density and pressure, Equation of State, TOV equation, energy conditions, Herrera's Causality and Cracking concept, adiabatic index and Harrison-Zel′dovich-Novikov static stability criteria. Section 6 contains mass-radius relation through which we can represent surface redshift of an anisotropic strange star. Lastly, in Section 7 we have drawn some concluding remarks on different aspects of the present model.

2. Basic Mathematical Formulation of Einstein's Spacetime

We consider static spherically symmetric spacetime metric through the line element

$$ds^2 = e^{\nu(r)}dt^2 - e^{\lambda(r)}dr^2 - r^2(d\theta^2 + \sin^2\theta d\phi^2), \tag{1}$$

where $\lambda(r)$ and $\nu(r)$ are metric function with TK type [1, 2], chosen as $\lambda(r) = \ln(1 + ar^2 + br^4)$ and $\nu(r) = Br^2 + 2\ln C$. Here a, b, B and C are arbitrary constants which can be evaluated on the basis of several physical requirements. These potentials are well behaved, satisfy the criteria for physical acceptance and free from the central singularity.

The energy-momentum tensor for anisotropic matter distribution, compatible with the spherically symmetric spacetime with signature (+, -, -, -), is given by

$$T_\nu{}^\mu = (\rho + p_r)\, u^\mu u_\nu + p_r g_\nu{}^\mu + (p_t - p_r)\, \eta^\mu \eta_\nu, \tag{2}$$

with $u^i u_j = -\eta^i \eta_j = 1$ and $u^i \eta_j = 0$. Here the vector u_i is the 4-velocity and η^i is the spacelike vector which is orthogonal to u_i. Here ρ, p_r and p_t are the matter density, radial pressure and tangential pressure respectively, of the fluid which is in orthogonal direction to p_r. Using Eqs. (1) and (2) one can obtain Einstein's field equations, assuming $G = c = 1$ (i.e. Geometrized unit), as follows

$$8\pi\rho = -e^{-\lambda}\left[\tfrac{1}{r^2} - \tfrac{\lambda'}{r}\right] + \tfrac{1}{r^2}, \tag{3}$$

$$8\pi p_r = e^{-\lambda}\left[\tfrac{\nu'}{r} + \tfrac{1}{r^2}\right] - \tfrac{1}{r^2}, \tag{4}$$

$$8\pi p_t = \tfrac{e^{-\lambda}}{4}\left[2\nu'' + \nu'^2 - \nu'\lambda' + \tfrac{2}{r}(\nu' - \lambda')\right], \tag{5}$$

where '$\prime$' denotes the derivatives of the respective parameters with respect to the radial parameter r.

The simplest phenomenological MIT bag model EOS [76, 26, 21] governs the SQM distribution inside the strange star. Considering that quarks are non-interacting, massless and including all the corrections of energy and pressure, the quark pressure of SQM can be defined as

$$p_r(r) = \sum_{f=u,d,s} p^f - B_g, \tag{6}$$

where p^f is the individual pressure of all three flavors of quarks and B_g is also known as vacuum energy density which can be treated as a constant quantity though recent research support its wide range of values.

The relation between the individual quark pressure p^f and energy density of individual quark flavor is given by $p^f = \frac{1}{3}\rho^f$. Therefore deconfined quarks inside the bag have the total energy ρ as follows

$$\rho = \sum_{f=u,d,s} \rho^f + B_g, \tag{7}$$

using Eqs. (6) and (7) we have the MIT bag EOS as

$$p_r(r) = \alpha\left[\rho(r) - 4B_g\right], \tag{8}$$

where α is a constant. Jasim et al. [75] considered $\alpha = 0.28$ for the massive strange quarks having mass 250 MeV [77], however for massless strange quarks, it has the value $\frac{1}{3}$ which we have considered in the present investigation for strange star. But we scientifically have studied it by finding out the values of B_g in terms of the mass-radius of different strange star candidates where depending on the values of these quantities it can be seen that B_g will change in a characteristic way.

Without involving any quantum mechanical particle aspect, this simplest EOS is very useful to study the equilibrium configuration of a compact star, in the framework of General Theory of Relativity, made up of only up, down and strange quarks. As we know the radial pressure must vanish at the surface so from Eq. (8) we have

$$\rho_R = 4B_g, \tag{9}$$

where R is the radius of the strange star and ρ_R is the surface density of the compact stellar model.

3. Solutions of the Field Equations

Now using Eq. (8) along with the metric functions ν and λ, we can solve Eqs. (3)-(5) and eventually we have the following solutions

$$\rho = \tfrac{3}{16}\tfrac{Bbr^4+Bar^2+2br^2+B+a}{\pi(br^4+ar^2+1)^2} + B_g, \tag{10}$$

$$p_r = \tfrac{1}{16}\tfrac{Bbr^4+Bar^2+2br^2+B+a}{\pi(br^4+ar^2+1)^2} - B_g, \tag{11}$$

$$p_t = \tfrac{1}{8}\tfrac{B^2br^6+B^2ar^4+B^2r^2+Bar^2-2br^2+2B-a}{\pi(br^4+ar^2+1)^2}. \tag{12}$$

The anisotropy (Δ) of our system reads as

$$\Delta \equiv (p_t - p_r) = \frac{(Br^2+\frac{3}{2})(Bbr^4+(Ba-2b)r^2+B-a)}{8\pi(br^4+ar^2+1)^2} + B_g. \tag{13}$$

The metric potentials can be expressed as

$$e^{\lambda(r)} = br^4 + ar^2 + 1, \tag{14}$$

$$e^{\nu(r)} = e^{Br^2+2\ln(C)}. \tag{15}$$

Variation of the metric potentials e^{ν} and e^{λ} are shown in Fig. 1 (upper and lower panel respectively) for various strange stars. From these graphical representations, it is very clear that $e^{\nu(r)}|_{r=0}$ is non zero positive value and $e^{\lambda(r)}|_{r=0} = 1$ which are the necessary conditions for the solution to be free from physical as well as geometric singularities. Both the metric potential are minimum at the centre, then increase nonlinearly and become maximum at the surface.

4. Bounds on the model parameters

4.1. Interior spacetime

The central density can be obtained from Eq. (10) as follows

$$\rho_c = \rho(r=0) = \frac{3}{16\pi}(B+a) + B_g. \tag{16}$$

Anisotropic condition states that, at the center ($r = 0$) anisotropy is zero, i.e., $p_r = p_t$,

$$p_r(r=0) = p_t(r=0). \tag{17}$$

4.2. Exterior spacetime

To find out the values of constants, we will match our interior spacetime with the exterior Schwarzschild metric [78] which is given by

$$ds^2 = \left(1-\frac{2M}{r}\right)dt^2 - \left(1-\frac{2M}{r}\right)^{-1}dr^2 - r^2(d\theta^2+\sin^2\theta d\phi^2), \tag{18}$$

where M is the total mass of the strange star.

At the boundary, i.e., $r = R$ where R is the radius of the corresponding star, metric coefficients g_{tt}, g_{rr} and $\frac{\partial g_{tt}}{\partial r}$ are continuous between the interior and exterior region which leads to the following conditions

$$g_{tt} : 1 - \frac{2M}{R} = e^{BR^2+2\ln C}, \tag{19}$$

$$g_{rr} : (1 - \frac{2M}{R})^{-1} = (1 + aR^2 + bR^4), \tag{20}$$

$$\frac{\partial g_{tt}}{\partial r} : \frac{M}{R^2} = BRe^{BR^2+2\ln C}. \tag{21}$$

Solving Eqs. (19)-(21), we can obtain the values of the constants a, b, B, C in terms of M and R as follows

$$a = -\frac{1}{2}\frac{M\,(8M^2 - 9MR + 4R^2)}{R^2(-R + 2M)(M^2 - MR + R^2)}, \tag{22}$$

$$b = \frac{4M^3 - 5M^2R}{4M^3R^4 - 6M^2R^5 + 6MR^6 - 2R^7}, \tag{23}$$

$$B = \frac{M}{R^2(R - 2M)}, \tag{24}$$

$$C = e^{\frac{(-R+2M)\ln\left(\frac{R-2M}{R}\right)+M}{-2R+4M}}. \tag{25}$$

At the surface (i.e., $r = R$) radial pressure vanishes, that gives

$$p_r(r = R) = \left[\frac{(BbR^4+BaR^2+2bR^2+B+a)}{16\pi(R^4b+R^2a+1)^2}\right] - B_g = 0. \tag{26}$$

Inserting the expressions for a, b, B in Eq. (26), B_g becomes

$$B_g = \frac{3M(2R - 3M)}{32\pi R^2(M^2 - MR + R^2)}. \tag{27}$$

Finally we have obtained all constants in terms of mass (M) and radius (R) of the strange star. Using observed values of these quantities we have calculated numerical values of different constants and physical parameters for various candidates of strange stars, shown in Tables 1 and 2.

5. Physical features of the proposed model

5.1. Density and pressure

Using density profile as expressed in Eq. (10) along with the numerical values of different constants, we are now able to plot the variation of $\rho(r)$

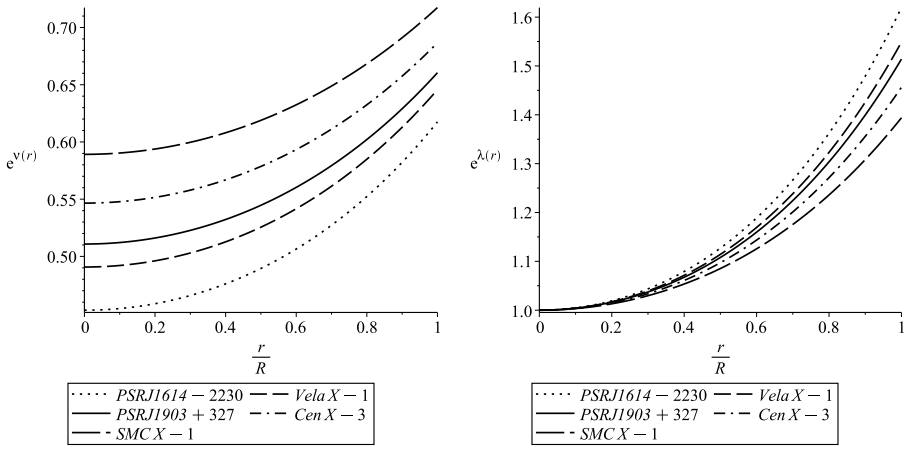


Figure 1: Variation of e^{ν} (left panel), e^{λ} (right panel) w.r.t. the fractional radial coordinate r/R for different strange star candidates.

with fractional radial coordinate r/R for the different strange star candidates. From Fig. 2, it is clear that density is finite at the center of the strange star and decreases monotonically with the increase of radius of the stellar body. If we look at the numerical values of central density and surface density of various candidates of strange stars in Table 1, then table transparently shows the much higher value of central density w.r.t. the density at the surface of the stars, which is the characteristic of ultra dense strange quark stars [50, 79, 80].

The radial pressure p_r and tangential pressure p_t are also expressed graphically using the numerical values of different constants. Their finite values at the center certify a singularity free model of strange star. From Fig. 2 we can see that radial pressure vanishes at the boundary of stars but tangential pressure dose not vanishes sharply at the surface of the star which indicate the spheroidal nature of the strange stars [81, 82, 74].

We have defined the anisotropy (Δ) of our model in Eq. (13). According to Hossein et al. [83], anisotropy will be directed outward when $\Delta > 0$ i.e., $p_t > p_r$, and inward when $\Delta < 0$ i.e., $p_t < p_r$. From Fig. 2 it is clear that anisotropy vanishes at the center of the star after that it remain negative upto certain distance. According to Hossain et al. [83], negative anisotropy allows the construction of massive stellar structure. It is very much prominent from the graphical representation that anisotropy will become positive after overcoming the negative value. According to Gokhroo and Mehra [84]

positive anisotropy helps to construct the more compact object. So our model acquire a stable configuration in the frame work of anisotropy. Also from the graphical representation we can see that the anisotropy increases and attain its maximum value at the surface of the star which is an inherent property of an ultra dense compact star [39].

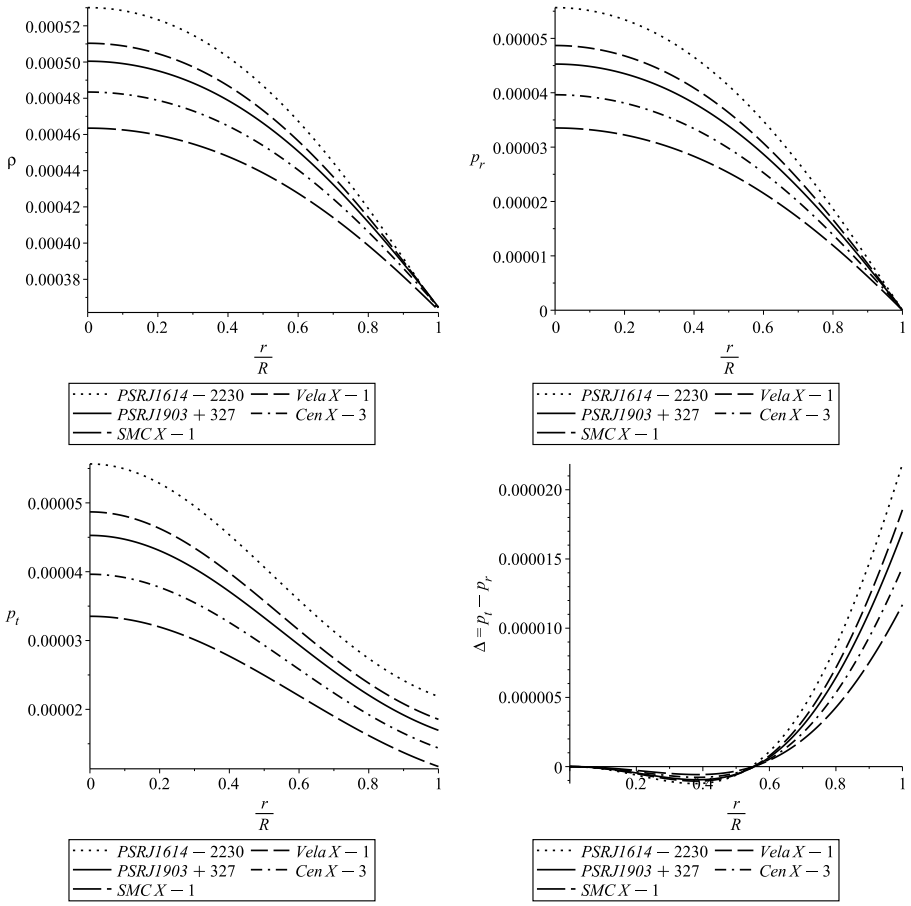


Figure 2: Variation of density (upper left), radial pressure (upper right), tangential pressure (lower left) and anisotropic stress (lower right) w.r.t. the fractional radial coordinate r/R for different strange star candidates.

5.2. Equation of State (EOS)

The radial (ω_r) and tangential (ω_t) EOS parameters for our system can be expressed as

$$\omega_r(r) = \frac{p_r}{\rho} = \frac{\alpha - 16\pi B_g(br^4+ar^2+1)^2}{3\alpha+16\pi B_g(br^4+ar^2+1)^2}, \tag{28}$$

$$\omega_t(r) = \frac{p_t}{\rho} = 2\frac{B^2r^2(br^4+ar^2+1) - Bar^2 - 2br^2 + 2B - a}{3\alpha+16\pi B_g(br^4+ar^2+1)}, \tag{29}$$

where, $\alpha = (Bbr^4 + Bar^2 + 2br^2 + B + a)$.

From Fig. 3 it is clear that $0 < \omega_i < \frac{1}{3}$ and decreases towards the surface of the respective stars. The inequality condition $0 < \omega_i < \frac{1}{3}$ indicate the non-exotic nature [73] of the underlying fluid distribution. Here we have considered the simplest barotropic EOS as $p_i = \omega_i\rho$, where ω_i are the EOS parameters along the radial and tangential directions. Here we have considered spatially homogeneous cosmic fluid. Though space and time dependence of ω are also possible which are in the following literature survey [85, 86, 87, 88].

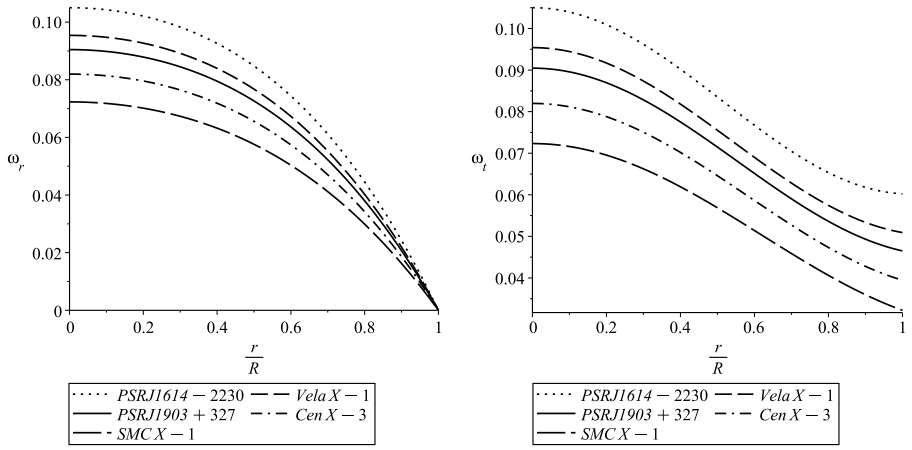


Figure 3: Variation of equation of state w_r (left panel) and w_t (right panel) w.r.t. the fractional radial coordinate r/R for different strange star candidates.

5.3. The generalised Tolman-Oppenheimer-Volkoff equation

To study the stability of a strange star under different forces we have to put our model under generalised Tolman-Oppenheimer-Volkoff (TOV) equation as proposed by Ponce de León [89], which can be represented as

$$-\frac{M_G(\rho+p_r)}{r^2}e^{\frac{\lambda-\nu}{2}} - \frac{dp_r}{dr} + \frac{2}{r}(p_t - p_r) = 0, \tag{30}$$

where $M_G = M_G(r)$ is the effective gravitational mass inside a sphere of radius r. $M_G(r)$ can be derived from the modified Tolman-Whittaker formula [90] as

$$M_G(r) = \frac{1}{2} r^2 e^{\frac{\nu-\lambda}{2}} \nu'. \tag{31}$$

Substituting this value in Eq. (30) we get the following form of TOV equation

$$-\frac{(\rho+p_r)\nu'}{2} - \frac{dp_r}{dr} + \frac{2}{r}(p_t - p_r) = 0. \tag{32}$$

The above equation explains the equilibrium conditions of the considered fluid sphere under the combined effect of gravitational, hydrostatic and anisotropic forces:

$$F_g + F_h + F_a = 0. \tag{33}$$

Here

$$F_g = -\frac{Br(Bbr^4+Bar^2+2br^2+B+a)}{4\pi(br^4+ar^2+1)^2}, \tag{34}$$

$$F_h = \frac{(Bbr^4+Bar^2+2br^2+B+a)(2br^3+ar)}{4\pi(br^4+ar^2+1)^3} - \frac{(2Bbr^3+Bar+2br)}{8\pi(br^4+ar^2+1)^2}, \tag{35}$$

$$F_a = \frac{[Bbr^4+(Ba-2b)r^2+B-a](Br^2+3/2)}{4\pi r(br^4+ar^2+1)^2} + \frac{2B_g}{r}. \tag{36}$$

The variations of different forces F_g, F_h and F_a are shown in Fig. 4. The profile tells us that the combined effect of hydrostatic force and anisotropic force is counter balanced by the gravitational force, as a result our considered ultra dense compact stars are in stable equilibrium situation.

5.4. Energy Conditions

In GR, the energy-momentum tensor T^{μ}_{ν} is described as mass, momentum and stress distribution caused by matter as well as any non-gravitational fields. However, the EFE is flexible enough about the acceptance of non-gravitational fields and states of matter in a spacetime model. Hence, the energy conditions represent and describe the common properties for various states of matter and all well-accepted non-gravitational fields in physics. At the same time, energy conditions are strong enough to rule out several EFE's solutions which are nonphysical in nature. To study the physical properties of an anisotropic strange star completely, we must have to check whether our model satisfies all the energy conditions or not. The energy conditions, viz. Null Energy Condition (NEC), Weak Energy Condition (WEC), Strong Energy Condition (SEC) and Dominant Energy Condition (DEC), are satisfied

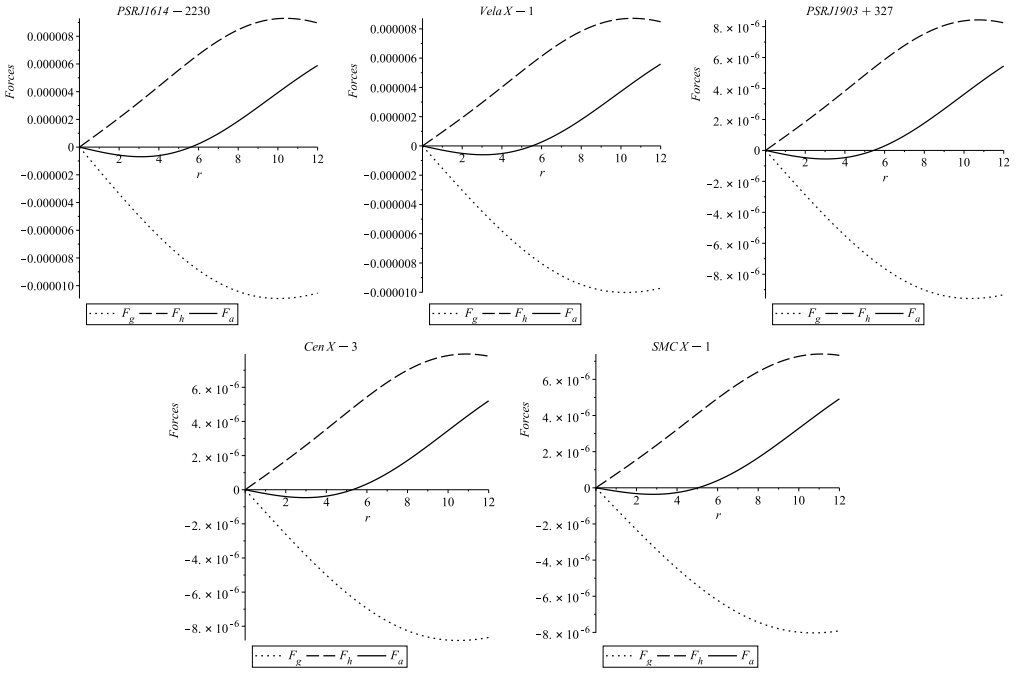


Figure 4: Variation of different forces w.r.t. the radial coordinate r for different strange star candidates.

if and only if the following inequalities hold simultaneously at every point inside the fluid sphere:

$$NEC \;:\; \rho \geq 0, \tag{37}$$

$$WEC \;:\; \rho + p_r \geq 0,\ \rho + p_t \geq 0, \tag{38}$$

$$SEC \;:\; \rho + p_r + 2p_t \geq 0, \tag{39}$$

$$DEC \;:\; \rho - |p_r| \geq 0,\ \rho - |p_t| \geq 0. \tag{40}$$

Though, there are several matter distributions, for which SEC is violated from mathematical prospect. According to Hawking [91], any cosmological inflationary process breaks SEC and for any scalar field along with a positive potential, this condition is not valid.

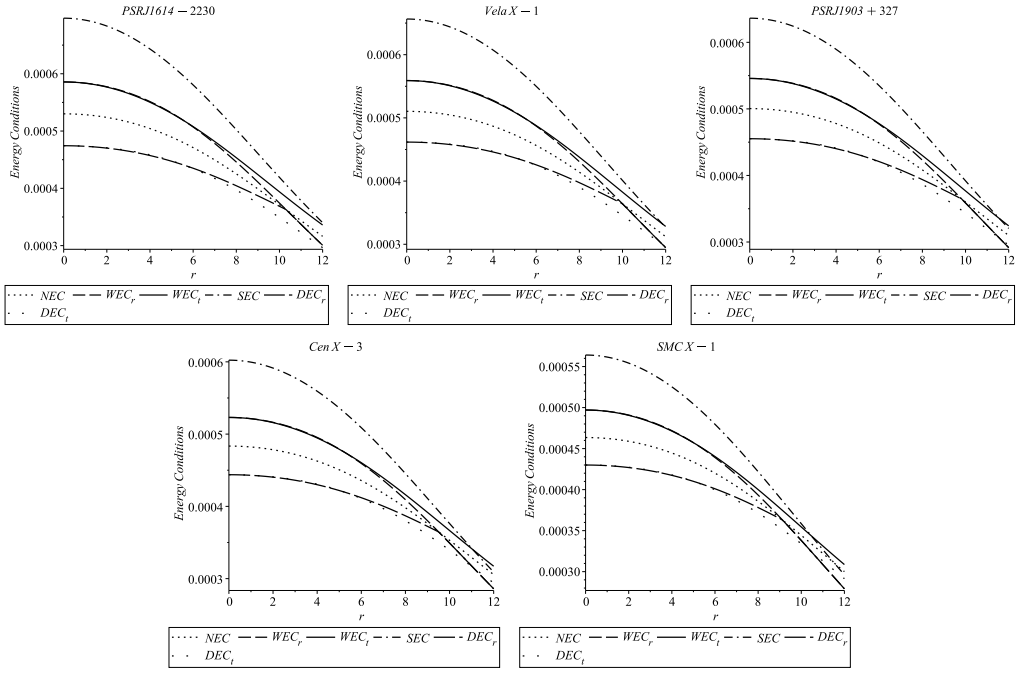


Figure 5: Variation of the different energy conditions w.r.t. the radial coordinate r for different strange star candidates.

Fig. 5 shows that our considered system with suitable choice of mass and radius, is consistent with all the energy conditions and confirms the physical validity of our model.

5.5. Herrera's condition for stability analysis

To study the stability of our stellar model, Herrera's causality condition and cracking concept [92, 93] are very much accepted over last three decade. According to the causality condition, square of the tangential (v_{ts}^2) and radial (v_{rs}^2) speed of sound should follow the restriction $0 \leq v_{rs}^2 \leq 1$ and $0 \leq v_{ts}^2 \leq 1$. Another concept tells us that the region for which square of the transverse speed of sound is smaller than the square of the radial speed of sound, is a potentially stable [92, 93, 94, 95, 96]. So, Herrera [93] and Andréasson [96] demand $|v_{rs}^2 - v_{ts}^2| \leq 1$ for stable matter distribution. This condition is known as 'no cracking', i.e., potentially stable region.

$$v_{rs}^2 = \frac{dp_r}{d\rho} = \frac{dp_r/dr}{d\rho/dr} = \frac{1}{3}, \tag{41}$$

$$v_{ts}^2 = \frac{dp_t}{d\rho} = \frac{dp_t/dr}{d\rho/dr} = \frac{2}{3}\frac{B^2b^2r^8+B^2abr^6+3Babr^4-6b^2r^4-B^2ar^2+X}{2Bb^2r^6+3Babr^4+6b^2r^4+Ba^2r^2+Y}, \tag{42}$$

where, $X = Ba^2r^2 + 8Bbr^2 - 6abr^2 - B^2 + 3Ba - 2a^2 + 2b$ and $Y = 2Bbr^2 + 6abr^2 + Ba + 2a^2 - 2b$.

$$\frac{dp_t}{d\rho} = \frac{dp_r}{d\rho} + \frac{d\Delta}{d\rho} = \frac{dp_r}{d\rho} + \frac{d\Delta/dr}{d\rho/dr}, \quad |v_{rs}^2 - v_{ts}^2| = |\frac{d\Delta/dr}{d\rho/dr}|. \tag{43}$$

Variations of v_{rs}^2 and v_{ts}^2 (Eqs. (41)-(42)) w.r.t. the fractional radial coordinate r/R, have been displayed in Fig. 6. Here graphs clearly show that both v_{rs}^2 and v_{ts}^2 remain within their specified range (0, 1) throughout the stellar body. In Fig. 6, magnitude of the difference between square of radial and tangential sound speed, i.e., $|v_{rs}^2 - v_{ts}^2|$ in Eq. (43), first decreases with the increasing radii and then bounces back to higher value, though always remain less than unity. Hence our model maintains the consistency with Herrera's cracking concept and re-establish the stable configuration.

5.6. Adiabatic Index

The term adiabatic index Γ, ratio of two specific heats [97], characterizes the stiffness of the EOS for a given density. We can use it to study the stability of relativistic and non relativistic fluid sphere. According to Bondi [98], for an anisotropic fluid sphere, Γ can be written as radial adiabatic index (Γ_r) and tangential adiabatic index (Γ_t). It is used to study the dynamical stability of the stellar system against an infinitesimal radial adiabatic perturbation [99, 100, 101, 102, 103, 104, 105, 106, 107]. For a stable Newtonian sphere,

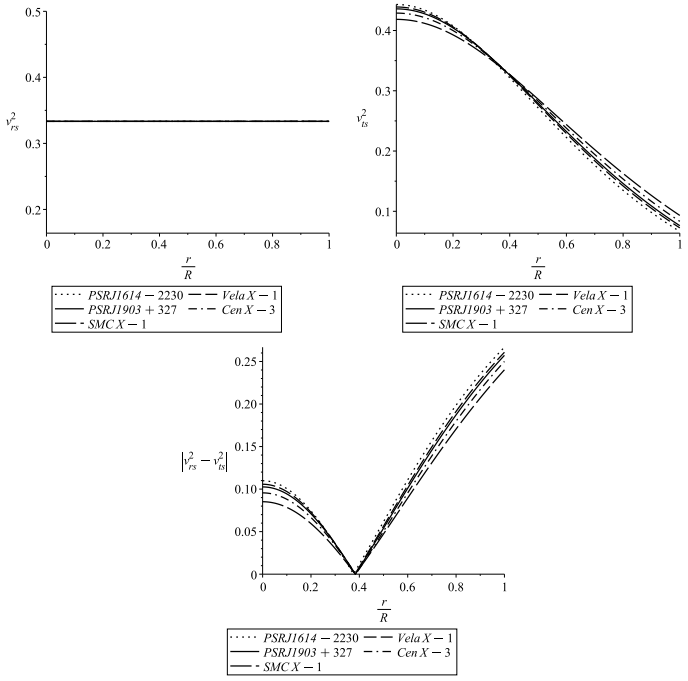


Figure 6: Variation of v_{rs}^2 (left panel), v_{ts}^2 (right panel) and $|v_{rs}^2 - v_{ts}^2|$ (lower panel) w.r.t. the fractional radial coordinate r/R for different strange star candidates.

the adiabatic index $\Gamma > \frac{4}{3}$ and in case of neutral equilibrium, $\Gamma = \frac{4}{3}$ according to Bondi [98]. For isotropic sphere in relativistic case, the above condition modifies due to the effect of regenerative pressure which leads the sphere to become more unstable. But for general relativistic anisotropic sphere, more complications arise because the nature of anisotropy decides the stability of the stellar system. The adiabatic index should exceed $\frac{4}{3}$ inside a dynamically stable, relativistic, anisotropic stellar system as predicted by Chan et al. [108], Heinzmann [109] and Hillebrandt [97]. For our proposed model the radial (Γ_r) and tangential (Γ_t) adiabatic indices can be defined as

$$\Gamma_r = \left[\frac{\rho(r)+p_r(r)}{p_r(r)}\right]\left[\frac{dp_r}{d\rho}\right] = \left[\frac{\rho(r)+p_r(r)}{p_r(r)}\right][v_{rs}^2]\,, \tag{44}$$

$$\Gamma_t = \left[\frac{\rho(r)+p_t(r)}{p_t(r)}\right]\left[\frac{dp_t}{d\rho}\right] = \left[\frac{\rho(r)+p_t(r)}{p_t(r)}\right][v_{ts}^2]\,. \tag{45}$$

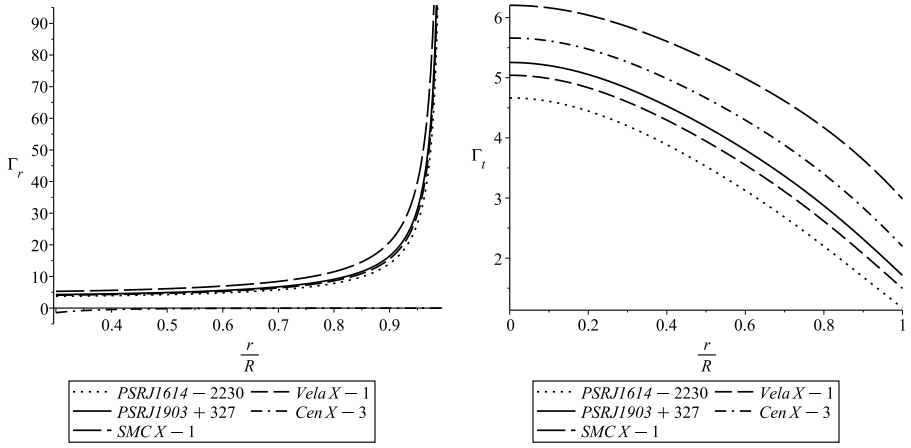


Figure 7: Variation of adiabatic index Γ_r (left panel) and Γ_t (right panel) w.r.t. the fractional radial coordinate r/R for different strange star candidates.

We have shown the graphical representation of radial and tangential adiabatic indices in Fig. 7. One can see that the adiabatic indices are greater than $\frac{4}{3}$ through out the stellar system and it represents a stable configuration against the radial perturbation.

5.7. Harrison-Zel′dovich-Novikov static stability criteria

To examine the stability of stars, Chandrasekhar [110], Harrison et al. [111] etc. calculate the eigen-frequencies for all the fundamental modes.

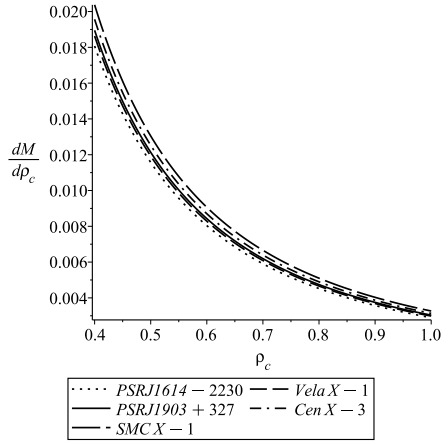


Figure 8: Variation of $\frac{dM}{d\rho_c}$ w.r.t. ρ_c for different strange star candidates.

Later, following Harrison et al. [111], Zel′dovich and Novikov [112] simplified the calculations. To make it simpler, they have presumed that adiabatic index for a pulsating star is comparable as for a slowly deformed matter. This presumption leads to the criteria that mass of the star must be increasing in nature with central density (i.e., $\frac{dM}{d\rho_c} > 0$) to achieve stable configuration and be unstable if $\frac{dM}{d\rho_c} < 0$.

In our proposed model, we can represent mass in terms of central density as follows

$$M(\rho_c) = \frac{R(-3R^2b + 16\pi B_g - 16\pi\rho_c + 3B)}{2(-3R^2b + 16\pi B_g - 16\pi\rho_c + 3B - \frac{3}{R^2})}. \tag{46}$$

Differentiating Eq. (46) w.r.t. ρ_c we get,

$$\frac{dM}{d\rho_c} = \frac{24\pi}{R\left(16\pi B_g - 3R^2b - 16\pi\rho_c + 3B - \frac{3}{R^2}\right)^2} > 0. \tag{47}$$

Fig. 8 also shows that $\frac{dM}{d\rho_c}$ is always positive throughout the stellar model. So, the Harrison-Zel′dovich-Novikov condition [73, 113] further confirms the stability of our proposed model.

6. Mass-Radius relation and surface redshift

For a static, spherically symmetric, anisotropic fluid distribution we can calculate its effective mass from the density profile, as given in Eq. (10) and

represent it graphically in Fig. 9. Hence, effective mass is

$$M_{eff} = \int_0^R 4\pi r^2 \rho(r) dr. \tag{48}$$

From Fig. 9, it is clear that as $r \to 0$, $M_{eff} \to 0$, so the effective mass is a monotonic increasing function.

For a static spherically symmetric perfect fluid star, Buchdahl [114] derived an upper limit for maximum allowed mass to radius ratio, i.e., $\frac{2M}{R} < \frac{8}{9}$. Mak et al. [115] generalised the result for charged sphere. The term $\frac{M}{R}$ is known as compactness which classifies the stellar objects into different categories as follows [116], (i) normal star: $M/R \sim 10^{-5}$, (ii) white dwarf: $M/R \sim 10^{-3}$, (iii) neutron star: $10^{-1} < M/R < 1/4$, (iv) ultra dense compact star: $1/4 < M/R < 1/2$ and (v) black hole: $M/R = 1/2$.

The compactness $u(r)$ for our model is given by

$$u(r) = \frac{M_{eff}}{r} = \frac{1}{r} \int_0^R 4\pi r^2 \rho(r) dr. \tag{49}$$

The graphical representation of compactness (Fig. 9) shows that it monotonically increases with the radius of the star and it's maximum value > 0.25, implies that our model corresponds to an ultra dense star.

The surface redshift (Z_s) and gravitational redshift (Z) for our model can be represented by the following relations

$$Z_s = \frac{1}{\sqrt{1-2u(r)}} - 1, \tag{50}$$

$$Z = e^{\frac{-\nu(r)}{2}} - 1. \tag{51}$$

In absence of cosmological constant, Barraco and Hamity [117] proved that $Z_s \leq 2$ for an isotropic star. Later Bohmer and Harko [118] established that or an anisotropic star, surface redshift can reach much higher value $Z_s \leq 5$, in presence of cosmological constant. Though the restriction was eventually modified and maximum acceptable value was calculated as $Z_s = 5.211$ [119]. In our case, we get $Z_s \leq 1$ for different strange star candidates (Table 2). The variation of the gravitational redshift w.r.t. r/R shown in Fig. 9, decreases monotonically with increasing radii. Z is positive as well as finite throughout the system, which strongly supports the acceptance of relativistic strange star model.

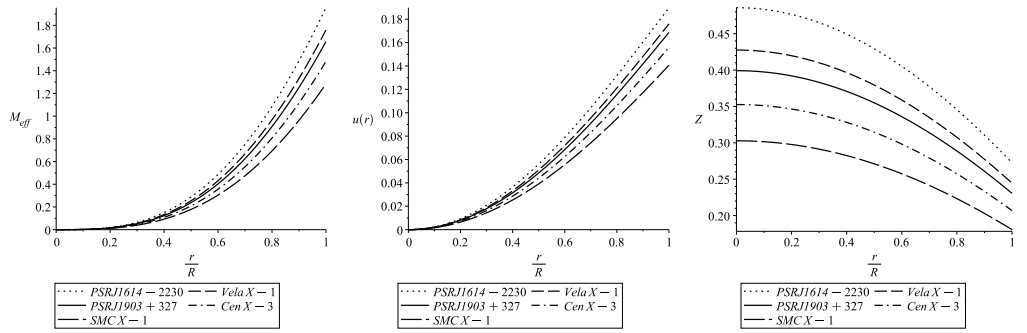


Figure 9: Variation of effective mass (left panel), compactification factor (middle panel) and gravitational redshift (right panel) w.r.t. the fractional radial coordinate r/R for different strange star candidates.

Table 1: Mass and radius of different strange star [120] candidates

Case	Stars	Mass (km)	Radius (km)	$\frac{M}{R}$	B_g (MeV/fm^3)	Z_s
I	$PSR\ J\ 1614\ 2230$	1.97	10.3	0.191	68.865	0.27
II	$Vela\ X-1$	1.77	9.99	0.177	69.097	0.24
III	$PSR\ J\ 1903+327$	1.667	9.82	0.17	69.161	0.23
IV	$Cen\ X-3$	1.49	9.51	0.157	69.144	0.21
V	$SMC\ X-1$	1.29	9.13	0.1413	68.84	0.18

Table 2: Determination of model parameters a, b, C, B, central density, surface density, radial pressure for different strange star candidates

Case	a (km^{-2})	b (km^{-4})	B (km^{-2})	C	$\rho(r=0)$ (gm/cm^3)	$\rho(r=R)$ (gm/cm^3)	$p_r(r=0)$ (dyne/cm^2)
I	0.004441	0.0000132	0.00292	0.6731	7.1713×10^{14}	4.912×10^{14}	6.753×10^{34}
II	0.004276	0.0000123	0.00275	0.7005	6.905×10^{14}	4.929×10^{14}	5.91×10^{34}
III	0.004193	0.0000118	0.00267	0.7147	6.771×10^{14}	4.933×10^{14}	5.493×10^{34}
IV	0.00405	0.000011	0.002523	0.7393	6.541×10^{14}	4.932×10^{14}	4.81×10^{34}
V	0.003883	0.0000101	0.00236	0.7676	6.271×10^{14}	4.91×10^{14}	4.067×10^{34}

7. Discussion and Conclusion

In the present article our motive is to explore the relevance of TK metric potentials in the modeling of strange quark stars. Considering the SQM distribution, expressed as the simplified MIT bag model EOS (Eq. (8)) we have studied the strange star more prominently. We have used Einstein's space-time to construct the preliminary mathematical background. From Einstein's field equations, Eqs. (3)-(5), by using the above mentioned TK metric potentials (Eqs. (14) and (15)) and MIT bag EOS (Eq. (8)), we have found out the solutions of various physical interest and also shown their variation graphically w.r.t. the radial distance r.

The metric potentials also specify the geometry of the space time. Their graphical representations (FIG. 1) tell us that both the metric potentials satisfy the necessary condition, i.e., $e^{\nu(r)}(r = 0)$ is non-zero positive and $e^{\lambda(r)}(r = 0) = 1$, so that the solutions should be free from physical and geometrical singularities. Both $e^{\nu(r)}$) and $e^{\lambda(r)}$ increase monotonically and non-linearly from centre to the surface for all the stars.

However in the framework of GR, our calculated value for B_g remains in the range $(55 - 75)$ MeV/fm^3, for stable SQM distribution [26, 21, 121], e.g. for star $PSRJ$ 1614 2230 (1.97 $M_\odot$ and $R = 10.3$ km) $B_g = 68.865$ MeV/fm^3, for star $PSR\,J$ 1903+327 (1.667 $M_\odot$ and $R = 9.82$ km) $B_g = 69.161$ MeV/fm^3 and for a relatively lower mass (1.29 $M_\odot$) star $SMC\ X - 1$ with radius $R = 9.13$ km, $B_g = 68.84$ MeV/fm^3. Hence it is fascinating to mention that our calculated B_g values satisfy not only the theoretical stability criteria [26, 21, 121] but also exactly match to the observational result of RHIC and CERN-SPS [27]. Our study may be generalised by considering more realistic EOS obtained from QCD simulations [122].

All the figures clearly establish the non-singular, stable nature from both geometrical, physical aspects. All the calculated values for different physical parameter are provided in Tables (1 and 2). Here, the important results from this strange star model have been discussed as follows:

1. Density and Pressure: Solving EFE (Eqs. (3)-(5)) we get the density (ρ), radial pressure (p_r) as well as tangential pressure (p_t) as shown in Eqs. (10)-(12) respectively. Central matter density ρ_c of Eq. (16) and central radial pressure (p_{rc}) can also be calculated by putting $r = 0$ in Eqs. (10) and (11). Density profile (ρ) and both the pressures (p_r and p_t) are free from central singularity. At the centre of the star ρ_c, p_r and p_t are finite and then decreases continuously with the increasing radius as shown in Fig. 2. In Ta-

ble (2) we have provided the values of density at the centre as well as at the surface for different strange stars. These numerical values give a clear idea that central density is higher than the surface density which is expected for an ultra dense star made of strange quark [50, 79, 80]. For example, in case of $PSR\ J\ 1614\ 2230$, $\rho_c \sim 7.1713 \times 10^{14}$ gm/cm^3 which reduces upto 68% at the surface, where density is 4.912×10^{14} gm/cm^3. Radial pressure at the centre of the star also very high, i.e., $(4.07 - 6.75) \times 10^{34}$ dyne/cm^2. According to Fig. 2, our model shows the spheroidal nature [81, 82, 74]. Variation of anisotropic stress w.r.t. the fractional radial coordinate r/R in Fig. 2 also establish the stable nature of our proposed model.

2. TOV equation: In our proposed model, generalised TOV Eq. (32) satisfies the stability criteria [89]. Fig. 4 clearly shows that combined effect of hydrostatic force (F_h) and anisotropic force (F_a) balances the effect of gravitational force (F_g). For every strange star candidates, we get almost same nature of force.

3. Energy conditions: Another strong reason behind the acceptability of our proposed model is that our model satisfies all the energy conditions, viz. NEC, WEC, SEC and DEC as mentioned in Eqs. (37)-(40). Graphical representations of these conditions, shown in Fig. 5 tell that all the energy values are maximum at the centre but reduces gradually towards the surface.

4. Stabilty of model: According to Herrera's [93] cracking concept, v_{rs}^2 and v_{ts}^2 should remain between the range 0 and 1. Here, following MIT bag model [Eq. (8)], v_{rs}^2 maintain a constant value $\frac{1}{3}$ throughout the stellar body and v_{ts}^2 in Eq. (42), always remain in the above mentioned range, which is clearly shown in Fig. 6. From graph (Fig. 6), v_{ts}^2 becomes maximum (≈ 0.45) at the centre and monotonically reduces towards the surface but always remains positive. For a potentially stable configuration, Herrera [93] and Andréasson [96] demand 'no cracking' condition i.e., $|v_{rs}^2 - v_{ts}^2| \leq 1$ to be obeyed and it is very clear from Fig. 6 that condition is also satisfied.

Both adiabatic index as defined in Eqs. (44) and (45) have been plotted in Fig. 7. From their variation it's clear that both Γ_r and $\Gamma_t \geq \frac{4}{3}$ at the centre and maintain Bondi's [98] criteria for static configuration throughout the total stellar body.

Another stability criteria is that, value of EOS parameter should lie in the range $0 - \frac{1}{3}$. Here, variation of both ω_r and ω_t have been featured graphically in Fig. 3. From figure it's clear that both ω_r, ω_t are positive through out the star and obtain maximum value (≈ 0.11) at the centre and reduces towards the surface area. Hence the fluid distribution is non-exotic [73] in nature.

Harrison-Zel′dovich-Novikov [111, 112] static stability criteria is also satisfied [Eq. (47)] for different strange stars in our proposed model. Fig. 8 undeniably shows that variation of $\frac{dM}{d\rho_c}$ is always remain positive within the entire stellar body and reduces towards the surface from maximum value at the centre similar as EOS parameter.

5. Buchdahl Condition: Fig. 9 shows the variation of effective mass function (M_{eff}) w.r.t. the fractional radial coordinate r/R. Variation shows that at $r \to 0$, $M_{eff} \to 0$, i.e., mass function is regular at the centre. According to Buchdahl [114] condition, mass radius ratio, i.e., $\frac{M}{R} \leq \frac{4}{3}$, for static, spherically symmetric and perfect fluid distribution. In the present study, we have considered 5 different strange star candidates (Table 1) with their observed radius and mass value, for which Buchdahl [114] condition is perfectly obeyed and the ratio remains in the range $(0.14 - 0.19)$.

6. Compactness and surface redshift: In this model, variation of compactness (u_r) and gravitational redshift (Z_s) have been displayed in Figs. 9. From figures it's clear that both the functions are continuous at $r \to 0$ and increases for higher r value for different strange stars. Calculated values for the surface redshift become maximum for star $PSR\ J\ 1614\ 2230$ ($Z_s = 0.27$) and $Z_s = 0.18$ for relatively low mass and smaller radius star $SMC\ X - 1$. Here the Z_s value strongly establish that our discussed candidates must be strange stars.

From literature survey, it's obvious that various group of researchers have studied strange stars in the framework of GR. But, few of them have introduced such a model that can't satisfy all the stability conditions at a time. Again few proposed models show the stability throughout the stellar system, but singularity arises at the centre. Few works do not satisfy all the stability criteria, energy conditions, Buchdahl limit [114] one at a time. However in our current study, using the TK metric and the EOS for MIT bag model under the framework of GR, we get a such a model that can overcome all the stability issues as well as exhibit the non-singular nature throughout the stellar body.

It is already mentioned, in a sketchy way, in Introduction that recently Jasim et al. [75] have studied anisotropic strange star using TK metric [1, 2]. In their study, they have assumed the value of bag constant as a 'fixed quantity', i.e., 60 MeV/fm^3 for all the strange star candidates under consideration with massive quark condition. As 'bag constant' is an inherent characteristics of strange stars so it can not be exactly same for different strange stars and hence the study by Jasim et al. [75] seems lacking for phys-

ical acceptance. However, from our model we can calculate the bag values for individual strange star, knowing their observed mass and radius only under the massless quark condition which fall within the proposed range $(55 - 75)$ MeV/fm^3 [26, 21]. Besides, our study provides more simplified solutions for ρ, p_r and p_t, using EFEs and MIT bag EOS. Jasim et al. [75] also have introduced the cosmological constant Λ which is zero in our case. Now, as a comparative study, we can observe that by setting only $\Lambda = 0$ in [75], one can not simply retrieve our results which are quite different from the results of Jasim et al. [75]. An overall observation on both the works reveals that the present investigation provides more general analysis of strange stars.

Hence an overall and final comment is that our proposed model is a representative of singularity-free, stable and viable one which represents a highly compact star made of SQM and perfectly fits for strange star candidates to analyze their different physically features.

Acknowledgement

SR and FR are thankful to the Inter University Centre for Astronomy and Astrophysics (IUCAA) for providing Visiting Associateship under which a part of this work has been carried out. SR also thanks the Centre for Theoretical Studies (CTS), IIT Kharagpur, India for providing short term visit under which rest of the work has been completed. SB is thankful to DST-INSPIRE (INDIA) [IF 160526] for financial support and all type of facilities for continuing research work. SB and DS acknowledge their gratitude to research scholar Shounak Ghosh for his valuable suggestions which became fruitful in preparation of the manuscript.

References

[1] R. C. Tolman, Phys. Rev. 8 (1939) 364.

[2] B. Kuchowicz, Acta Phys. Pol. 33 (1968) 541.

[3] A. Einstein, Sitzungsber. Preuss. Akad. Wiss 44 (1915) 778; ibid. 46 (1915) 799; ibid. 48 (1915) 844.

[4] A. Einstein, Ann. Phys. 17 (1905) 891.

[5] J.A. Wheeler, Geometrodynamics, Academic, New York, p.25 (1962).

[6] F. Wilczek, Phys. Today 52 (1999) 11.

[7] A. Hewish, S. J. Bell, J. D. H. Pilkington, P. F. Scott, and R. A. Collins, Nature 217 (1968) 709.

[8] P.B. Demorest, T. Pennucci, S.M. Ransom, M.S.E. Roberts, and J.W.T. Hessels, Nature 467 (2010) 1081.

[9] R. C. Duncan and C. Thompson, Astrophys. J. 392 (1992) L9.

[10] C. Thompson and R. C. Duncan, Astrophys. J. 473 (1996) 322.

[11] A. I. Ibrahim, S. Safi-Harb, J. H. Swank, W. Parke, and S. Zane, Astrophys. J. 574 (2002) L51.

[12] S. Chakrabarty, D. Bandyopadhyay, and S. Pal, Phys. Rev. Lett. 78 (1997) 2898.

[13] A. A. Isayev and J. Yang, Phys. Rev. C 69 (2004) 025801.

[14] A. A. Isayev, Phys. Rev. C 74 (2006) 057301.

[15] T. Tatsumi, Phys. Lett. B 489 (2000) 280.

[16] A. G. W. Cameron, Astrophys. J. 130 (1959) 916.

[17] N. Itoh, Prog. Theor. Phys. 44 (1970) 291.

[18] A. Bodmer, Phys. Rev. D 4 (1971) 1601.

[19] E. Witten, Phys. Rev. D 30 (1984) 272.

[20] P. Haensel, J. Zdunik, and R. Schaeffer, Astron. Astrophys. 160 (1986) 121.

[21] C. Alcock, E. Farhi, and A. Olinto, Astrophys. J. 310 (1986) 216.

[22] G. Pagliara, M. Herzog, and F. K. Röpke, Phys. Rev. D 87 (2013) 103007.

[23] A. Bauswein et al., Phys. Rev. Lett. 103 (2009) 011101.

[24] A. Bauswein, R. Oechslin, and H.-T. Janka, Phys. Rev. D 81 (2010) 024012.

[25] A. Chodos, R. L. Jaffe, K. Johnson, C. B. Thorn, and V. F. Weisskopf, Phys. Rev D, 9 (1974) 3471.

[26] E. Farhi and R. L. Jaffe, Phys. Rev. D 30 (1984) 2379.

[27] G. F. Burgio, M. Baldo, P. K. Sahu, and H. J. Schulze, Phys. Rev. C 66 (2002) 025802.

[28] A. Aziz, S. Ray, F. Rahaman, M. Khlopov and B. K. Guha, IJMPD 28 (2019) 1941006.

[29] G. Lugones and J. D. V. Arbañil, Phys. Rev. D 95 (2017) 064022.

[30] J. D. V. Arbañil and M. Malheiro, JCAP 11 (2016) 012.

[31] G. Abbas, S. Qaisar, and A. Jawad, Astrophys. Space Sci. 359 (2015) 57.

[32] A. A. Isayev, Phys. Rev. C 91 (2015) 015208.

[33] L. Paulucci and J. E. Horvath, Phys. Lett. B 733 (2014) 164.

[34] J. Madsen, Lect. Notes Phys. 516 (1999) 162.

[35] J. Madsen, J. Phys. G 28 (2002) 1737.

[36] M. Alford, K. Rajagopal, and F. Wilczek, Nucl. Phys. B 537 (1999) 433.

[37] R. Rapp, T. Schaefer, E. V. Shuryak, and M. Velkovsky, Ann. Phys. 280 (2000) 35.

[38] G. Lugones and J.E. Horvath, Phys. Rev. D 66 (2002) 074017.

[39] D. Deb, S. Roy Chowdhury, S. Ray, F. Rahaman, and B. K. Guha, Ann. Phys. (Amsterdam) 387 (2017) 239 .

[40] M. K. Mak and T. Harko, Chin. J. Astron. Astrophys. 2 (2002) 248.

[41] F. Rahaman, R. Sharma, S. Ray, R. Maulick, and I. Karar, Eur. Phys. J. C 72 (2012) 2071.

[42] D. Deb, B. K. Guha, F. Rahaman, and S. Ray, Phy. Rev. D 97 (2018) 084026.

[43] D. Deb, F. Rahaman, S. Ray, and B. K. Guha, J. Cosmol. Astropart. Phys. 03 (2018) 044.

[44] S. Biswas, S. Ghosh, B. K. Guha, F. Rahaman, and S. Ray, Ann. Phys. 401 (2019) 1(20).

[45] K. D. Krori and J. Barua, J. Phys. A: Math. Gen. 8 (1975) 508.

[46] M. Brilenkov, M. Eingorn, L. Jenkovszky, and A. Zhuk, J. Cosmol. Astropart. Phys. 08 (2013) 002.

[47] S. D. Maharaj, J. M. Sunzu, and S. Ray, Eur. Phys. J. Plus. 129 (2014) 3.

[48] N. R. Panda, K. K. Mohanta, and P. K. Sahu, J. Phy.: Conf. Ser. 599 (2015) 012036.

[49] P. Bhar, Astrophys. Space Sci. 357 (2015) 46.

[50] R. Ruderman, Ann. Rev. Astron. Astrophys. 10 (1972) 427.

[51] R. L. Bower and E. P. T. Liang, Astrophys. J. 188 (1974) 657.

[52] S. S. Bayin, Phys. Rev. D, 26 (1982) 1262.

[53] S. D. Maharaj and R. Maartens, Gen. Relativ. Gravit. 21 (1989) 899.

[54] R. Kippenhahn and A. Weigert, Stellar Structure and Evolution, Springer, Berlin (1990).

[55] R. F. Sawyer, Phys. Rev. Lett. 29 (1972) 382.

[56] A. I. Sokolov, JETP Lett. 79 (1980) 1137.

[57] F. Weber, Pulsars as Astrophysical Observatories for Nuclear and Particle Physics, Institute of Physics Publishing, Bristol (1999).

[58] V. V. Usov, Phys. Rev. D 70 (2004) 067301.

[59] K. Krori, P. Bargohain, and R. Devi, Can. J. Phys. 62 (1984) 239.

[60] B. V. Ivanov, Phys. Rev. D 65 (2002) 104011.

[61] F. E. Schunck and E. W. Mielke, Class. Quant. Gravit. 20 (2003) 301.

[62] M. K. Mak and T. Harko, Proc. R. Soc. A 459 (2003) 393.

[63] V. Varela, F. Rahaman, S. Ray, K. Chakraborty, and M. Kalam, Phys. Rev. D 82 (2010) 044052.

[64] F. Rahaman, S. Ray, A. K. Jafry, and K. Chakraborty, Phys. Rev. D 82 (2010) 104055.

[65] F. Rahaman, P. K. F. Kuhfittig, M. Kalam, A. A. Usmani, and S. Ray, Class. Quant. Gravit. 28 (2011) 155021.

[66] S. K. Maurya and Y. K. Gupta, Phys. Scr. 86 (2012) 025009.

[67] M. Kalam et al., Eur. Phys. J. C 72 (2012) 2248.

[68] F. Rahaman, R. Maulick, A. K. Yadav, S. Ray, and R. Sharma, Gen. Relativ. Gravit. 44 (2012) 107.

[69] S. K. Maurya, Y. K. Gupta, S. Ray, and B. Dayanandan, Eur. Phys. J. C 75 (2015) 225.

[70] M. Malaver, Open Sci. J. Mod. Phys. 2 (2015) 65.

[71] N. Pant, N. Pradhan, M. H. Murad, and M. Malaver, Am. J. Sci. Tehnol. 2 (2015) 43.

[72] S. K. Maurya, Y. K. Gupta, S. Ray, and D. Deb, Eur. Phys. J. C 76 (2016) 693.

[73] D. Shee, F. Rahaman, B. K. Gupta, and S. Ray, Astrophys. Space Sci. 361 (2016) 167.

[74] D. Shee, S. Ghosh, F. Rahaman, B. K. Gupta, and S. Ray, Astrophys. Space Sci. 362 (2017) 114.

[75] M. K. Jasim, Y. K. Gupta, S. Ray, D. Deb, and S. Roy Chowdhury, Eur. Phys. J. C 78 (2018) 603

[76] A. Chodos, R. L. Jaffe, K. Johnson, C. B. Thorn, and V. F. Weisskopf, Phys. Rev. D 9 (1974) 3471.

[77] N. Stergioulas, Living Rev. Relativ. 6 (2003) 3.

[78] K. Schwarzschild, Sitz. Deut. Akad. Wiss. Math. Phys. (Berlin) 23 (1916) 189.

[79] N. K. Glendenning, Compact Stars: Nuclear Physics, Particle Physics and General Relativity, Springer, New York, (1997) pp. 468.

[80] M. Herzog and F. K. Röpke, Phys. Rev. D 84 (2011) 083002.

[81] H. Quevedo, Phys. Rev. D 39 (1989) 2904.

[82] E. N. Chifu, Abra. Zelm. J. 5 (2012) 31.

[83] Sk. M. Hossein, F. Rahaman, J. Naskar, M. Kalam, and S. Ray, Int. J. Mod. Phys. D 21 (2012) 1250088.

[84] M. K. Gokhroo and A. L. Mehra, Gen. Relativ. Gravit. 26 (1994) 75.

[85] S. V. Chervon and V. M. Zhuravlev, Zh. Eksp. Teor. Fiz. 118 (2000) 259.

[86] V. M. Zhuravlev, Zh. Eksp. Teor. Fiz. 120 (2001) 1042.

[87] P. J. E. Peebles and B. Ratra, Rev. Mod. Phys. 75 (2003) 559.

[88] A. A. Usmani, P. P. Ghosh, U. Mukhopadhyay, P. C. Ray, and S. Ray, Mon. Not. R. Astron. Soc. 386 (2008) L92.

[89] Ponce de León, J.: Gen. Relativ. Gravit. 19 (1987) 797.

[90] J. Devitt and P. S. Florides, Gen. Relativ. Gravit. 21 (1989) 585.

[91] S. Hawking, G. F. R. Ellis, The Large Scale Structure of Space-Time, Cambridge University Press, Cambridge (1973).

[92] L. Herrera, G. Ruggeri, and L. Witten, Astrophys. J. 234 (1979) 1094.

[93] L. Herrera, Phys. Lett. A 165 (1992) 206.

[94] R. Chan, L. Herrera, and N. O. Santos, Mon. Not. R. Astron. Soc. 265 (1993) 533.

[95] H. Abreu, H. Hernández, and L.A. Núñez, Class. Quant. Gravit. 24 (2007) 4631.

[96] H. Andréasson, Commun. Math. Phys. 288 (2009) 715.

[97] W. Hillebrandt and K.O. Steinmetz, Astron. Astrophys. 53 (1976) 283.

[98] H. Bondi, Proc. R. Soc. Lond. A 281 (1964) 39.

[99] S. Chandrasekhar, Astrophys. J. 140 (1964) 417.

[100] J. M. Bardeen, K. S. Thorne, and D. W. Meltzer, Astrophys J. 145 (1966) 505.

[101] R. M. Wald, General Relativity (Chicago Press, Chicago and London, (1984) pp. 127.

[102] H. Knutsen, Mon. Not. R. Astron. Soc. 232 (1988) 163.

[103] L. Herrera and N.O. Santos, Phys. Rep. 286 (1997) 53.

[104] D. Horvat, S. Ilijíc, and A. Marunovíc, Class. Quant. Gravit. 28 (2011) 025009.

[105] D. D. Doneva and S. S. Yazadjiev, Phys. Rev. D 85 (2012) 124023.

[106] M. K. Mak and T. Harko, Eur Phys. J. C 73 (2013) 2585.

[107] H. O. Silva, C. F. B. Macedo, E. Berti, and L. C. B. Crispino, Class. Quant. Gravit. 32 (2015) 145008.

[108] R. Chan, L. Herrera, and N. O. santos, Mon. Not. R. Astron. Soc. 265 (1993) 533.

[109] H. Heintzmann and W. Hillebrandt, Astron. Astrophys. 24 (1975) 51.

[110] S. Chandrasekhar, Phys. Rev. Lett. 12 (1964) 114.

[111] B. K. Harrison, K. S. Thorne, M. Wakano, and J. A. Wheeler, Gravitational Theory and Gravitational Collapse, Chicago, University of Chicago Press (1965).

[112] Ya. B. Zel′dovich and I. D. Novikov, Relativistic Astrophysics Vol. 1: Stars and Relativity, Chicago, University of Chicago Press (1971).

[113] P. Bhar, K. N. Singh, F. Rahaman, N. Pant, and S. Banerjee, Int. J. Mod. Phys. D 26 (2017) 15.

[114] H. A. Buchdahl, Phys. Rev. 116 (1959) 1027.

[115] M. K. Mak, P. N. Dobson and T. Harko, Europhys. Lett. 55 (2001) 310.

[116] K. Jotania and R. Tikekar, Int. J. Mod. Phys. D 15 (2006) 1175.

[117] D. E. Barraco and V. H. Hamity, Phys. Rev. D. 65 (2002) 124028.

[118] C. G. Bohmer and T. Harko, Class. Quant. Gravit. 23 (2006) 6479.

[119] B. V. Ivanov, Phys. Rev. D 65 (2002) 104011.

[120] F. Rahaman, K. Chakraborty, P. K. F. Kuhfittig, G. C. Shit, and M. Rahman, Eur. Phys. J. C 74 (2014) 3126.

[121] F. Weber, Prog. Part. Nucl. Phys. 54 (2005) 193.

[122] M. G. Alford, S. Han and M. Prakash, Phys. Rev. D 88 (2013) 083013.